The Corrected Allan Variance: Stability Analysis of Frequency Measurements with Missing Data

L. Galleani and I. Sesia, "The Corrected Allan Variance: Stability Analysis of Frequency Measurements With Missing Data," *IEEE Trans. Ultra. Ferro. Freq. Contr.*, vol. 66, no. 10, pp. 1667-1683, October 2019

The Corrected Allan Variance: Stability Analysis of Frequency Measurements With Missing Data

Lorenzo Galleani, *Senior Member, IEEE,* and Ilaria Sesia, *Member, IEEE*

***Abstract*—Atomic clocks are essential elements in a variety of applications, such as global navigation satellite systems. Consequently, monitoring their performances is fundamental. The Allan variance is the key statistical tool for the performance characterization of atomic clocks. This article proves that the Allan variance computed from frequency measurements with missing data is affected by a bias which can make it dramatically different from the expected behavior in the full data case. Furthermore, it shows how to eliminate (or largely reduce) this bias by correcting the Allan variance. The corrected Allan variance is obtained for some of the most common atomic clock noise components, and it is validated through numerical simulations.**

TIPS: VII (e) - Category: *FREQUENCY CONTROL* - Subcategory: *Frequency measurement and statistics*.

I. Introduction

Atomic clocks play a key role in many applications, such as global navigation satellite systems (GNSS). In GNSSs, such as the global positioning system (GPS) and Galileo, position is estimated from the measurements of the time of flight of the signals travelling from the system satellites to the receiver, and hence an error in time results in an error in position. An accurate characterization of the atomic clocks performances is therefore fundamental. The key quantity for the performance characterization of an atomic clock is frequency stability, whose standard measure is the Allan variance [1]-[4]. The Allan variance can be evaluated from the measurements of the time deviation of the clock with respect to a time reference, or, equivalently, from frequency deviation measurements. In some cases, such as for optical clocks and primary frequency standards, only frequency measurements are available.

Unfortunately, missing data are common. Data can be missing for several reasons. First, the clock may not be always working properly, as happens, for example, with optical clocks, which exhibit unprecedented stability performances but are still not reliable as cesium or rubidium clocks. Second, in space applications the clock measurements may not be available all the time due to satellite maintenance operations, or the satellite may not be visible all the time. For example, in the atomic clock ensemble in space (ACES) experiment [5], the atomic clocks onboard the international space station (ISS) will be visible for approximately 5 minutes of the ISS pass, out of 90 minutes of its orbital period, resulting in approximately 94% of missing data. Third, particularly in pre-processing, it might be necessary to remove data with anomalous behaviors, such as outliers [6], which could otherwise spoil the clock performance analysis.

Although missing data are common and sometimes represent a challenging percentage of the total available data, it is still fundamental to compute the Allan variance and characterize the clock stability, because of its central role in the clock performance characterization. This article shows two things. First, that the Allan variance for frequency measurements with missing data can have a strong bias, namely, it can be profoundly different from its expected behavior. Second, how to remove this bias by correcting the Allan variance.

Before summarizing these results and illustrating the structure of the article, it is fundamental to review the concept of bias, a key quantity in estimation theory [7]. Suppose that the temperature of a human body is measured. Assume that $y = 37$ °C is the true temperature value. The measurements are obtained by using a thermometer which produces the estimates $\hat{y}_1 = 36.2$ °C, $\hat{y}_2 = 35.8$ °C, $\hat{y}_3 = 36.1$ °C, … The corresponding estimation errors are $e_1 = \hat{y}_1 - y = -0.8$ °C, $e_2 = -1.2$ °C, $e_3 = -0.9$ °C, … The estimates $\hat{y}_1$, $\hat{y}_2$, $\hat{y}_3$, …, can be modeled as the realizations of a random variable $\hat{Y}$, referred to as the estimator. Also the estimation errors e_1, e_2, e_3, …, can be modeled as the realizations of a random variable $\epsilon = \hat{Y} - y$. In the considered example, one averages all of the (infinite) measurements and obtains $E[\hat{Y}] = 36$ °C. The average estimation error $B = E[\epsilon] = E[\hat{Y}] - y = -1$ °C is referred to as bias. Since $B \neq 0$, the estimator $\hat{Y}$ is said to be biased. This bias might be due to the fact that the thermometer was inadvertently placed on the fabric of the vest, rather than directly on the skin. If the thermometer is correctly placed on the skin, the body temperature estimator $\hat{Y}$ returns, on the average, $E[\hat{Y}] = 37$ °C, therefore $B = 0$ and the estimator is unbiased. Summarizing, the estimates produced by an unbiased estimator fluctuate about the true value, whereas the estimates produced by a biased estimator fluctuate about a value different from the true value.

When full time or frequency measurements are used, the Allan variance estimator is unbiased, and the estimates of the Allan variance fluctuate about the true value, namely, the Allan variance as defined by Allan in 1966 [1]. The Allan variance estimator is still unbiased when time measurements with missing data are considered, as proved in Appendix 4. For this case, an effective estimator which takes into account long blocks of missing data and outliers is developed in [8]. Conversely, when frequency measurements with missing data are used, the Allan variance estimates fluctuate with respect to a value different from the true Allan variance, and the estimator is biased. For example, Fig. 1 shows Allan deviation estimates (thin blue lines) obtained from $N = 540$ frequency

L. Galleani is with Politecnico di Torino, Corso Duca degli Abruzzi 24, 10129 Torino, Italy (email: galleani@polito.it).

I. Sesia is with INRIM, Strada delle Cacce 91, 10135 Torino (email: i.sesia@inrim.it).

measurements of a white frequency modulation (WFM) noise, and the corresponding Allan deviation (dashed blue line), obtained by averaging an infinite number of estimates, or, equivalently, by analytic calculations. The thin black lines represent instead Allan deviation estimates obtained from the previous frequency measurements when 94% of data are removed, with the pattern of regularly missing data blocks described at the beginning of Sect. IV-A, and similar to the ACES experiment previously discussed. The estimates fluctuate about an Allan deviation (dashed black curve) which is dramatically different from the expected true value. Therefore, the Allan variance estimator is biased for frequency measurements with missing data. Unfortunately, when data are missing, it is not possible to recover time measurements from frequency measurements [9], and one cannot use the estimator developed in [8]. Nevertheless, this article shows how to define a corrected Allan variance which corresponds to the expected true value, and whose estimator is consequently unbiased. The proposed method can be used for any pattern of missing data, and, moreover, it does not replace the missing data by using, for example, interpolation techniques, as in [10]. Note that, because of the way the Allan variance is defined, the correction can be computed in a given observation interval region only if the dominant noise component in that region is known. The advantage of the corrected Allan variance is that it provides an estimate of the level of the dominant noise component in every observation interval region, which is the key parameter for the assessment of the clock stability performances.

The corrected Allan variance is developed for a WFM, a white phase modulation (WPM), and a random walk frequency modulation (RWFM), three of the most common noise components of atomic clocks [11]. The developed method can be used also when multiple noise components are present. Note that, as commonly done in stability analysis, the method assumes that deterministic components, such as frequency drifts, have been removed from the data. Nonstationary behaviors, such as clock anomalies, typically increase the Allan variance and reduce the stability performances, as happens, for instance, in presence of a sinusoidal term, which generates bumps in the Allan variance. This behavior occurs also when missing data are present. On one hand, to avoid pessimistic estimates of the clock stability, nonstationary behaviors due to known causes, such as maintanaince operations, should be removed from frequency measurements before computing the corrected Allan variance. On the other hand, to avoid optimistic estimates of the clock stability, anomalous nonstationarity behaviors not corresponding to known causes, should not be removed, but rather revealed and characterized with the dynamic Allan variance (DAVAR) [12]-[15], a sliding Allan variance which produces a surface function of time and the observation interval. This surface changes with time when an anomaly occurs. When data are missing, to reveal and characterize such nonstationary clock behaviors, one can slide the corrected Allan variance on the data, therefore obtaining a corrected DAVAR.

The corrected Allan variance is validated on simulated frequency measurements both for individual noise components and for multiple noise components. For individual noise components, the cases of regularly spaced blocks of missing data and uniformly distributed missing data are considered. This second case is interesting because in the recent years the Allan variance has been spreading out to a variety of fields other than precise timing, and patterns of missing data are common in many applications. The results show that the corrected Allan variance completely removes the bias. For multiple noise components, the cases of WPM plus WFM, WPM plus RWFM, and WFM plus RWFM are considered, first for regularly spaced blocks of missing data, and then, for the case of WPM plus WFM, also for blocks of missing data with random positions. In all of these cases, the corrected Allan variance either removes, or largely reduces, the bias. Additional results show that, when the wrong dominant noise components are chosen, the corrected Allan variance does not satisfy the properties expected from a clock stability measure, and this fact can be used to detect a model mismatch.

Note that the basic idea behind the method presented in this article is sketched in the conference paper [16]. Specifically, [16] shows that a correction factor is needed to eliminate the bias of the Allan variance, but it does not derive it. The present article derives instead the correction factor for WFM, WPM, RWFM, and it also discusses the case of multiple noise components. Furthermore, it obtains the correction factor through a matrix calculus technique which allows a straightforward software implementation. Finally, [16] shows simulation results for WFM only, whereas the present article shows simulation results for WFM, WPM, RWFM, and for multiple noise components.

The article is organized as follows. Section II discusses the standard definition of the Allan variance for frequency measurements, first for the case of a complete data set, and then for the case of missing data. Then, Sect. III introduces the corrected Allan variance for WFM, WPM, and RWFM, and discusses its estimation for multiple noise components. Finally, Sect. IV validates the proposed method on simulated data, both for individual and multiple noise components.

II. The Allan Variance

This section first reviews the classical definition of the Allan variance in the case of full data for WFM, WPM, and RWFM. Then, it shows the proposed modified definition for the case of missing data.

A. Full Data

The Allan variance is defined as [1], [2]

$$\sigma_y^2(\tau) = \frac{1}{2}\left\langle (\bar{y}(t+\tau) - \bar{y}(t))^2 \right\rangle \tag{1}$$

where τ is the observation interval, $\langle\rangle$ indicates an average over the entire time axis, and the average frequency deviation $\bar{y}(t)$ is defined as

$$\bar{y}(t) = \frac{1}{\tau}\int_{t-\tau}^{t} y(t')dt' \tag{2}$$

The quantity $y(t)$ is the normalized frequency deviation, defined as

$$y(t) = \frac{\nu(t) - \nu_0}{\nu_0} \tag{3}$$

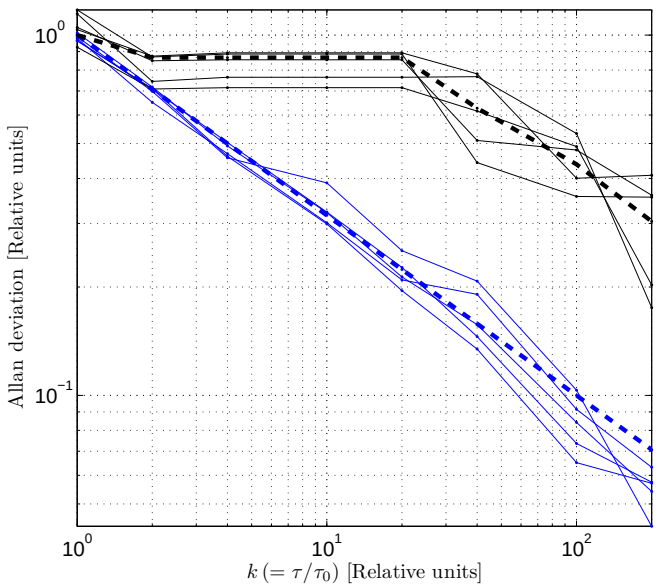

Fig. 1. Bias of the Allan deviation computed from frequency measurements with missing data. The dashed blue curve represents the theoretical Allan deviation for a WFM when all of the frequency measurements are available. This Allan deviation follows the expected $k^{-1/2}$ behavior, and it can be obtained either from analytic calculations, or by averaging an infinite number of estimates. The solid blue curves represent a few of such estimates, obtained from $N = 540$ WFM data. These estimates fluctuate about the Allan deviation for full data. When 94% of the data are removed with the pattern of missing data blocks described at the beginning of Sect. IV-A, the Allan deviation for missing data (dashed black curve) shows a large difference, or bias, with respect to the Allan deviation for full data. The corresponding estimates of the Allan deviation in the missing data case (solid black curves) fluctuate about this biased Allan deviation. Note that the Allan variance for missing data, and its estimator, can be seen as approximations of the Allan variance for full data, and its estimator, where the approximaton error is the bias. This bias, or approximation error, is due to the fact that the Allan variance for missing data is computed by using only the available frequency measurements.

where ν_0 is the nominal frequency of the clock, and $\nu(t)$ its instantaneous frequency. The normalized frequency deviation $y(t)$ is connected to the time deviation $x(t)$ through the relationship

$$y(t) = \frac{dx(t)}{dt} \tag{4}$$

In practical applications, it is common to use sampled average frequency measurements defined as

$$y[n] = \frac{1}{\tau_0}\int_{(n-1)\tau_0}^{n\tau_0} y(t')dt' \tag{5}$$

where τ_0 is the sampling time, and $n = t/\tau_0$ is discrete time. By using (4), frequency measurements can be written with respect to time measurements as

$$y[n] = \frac{x[n] - x[n-1]}{\tau_0} \tag{6}$$

where $x[n] = x(n\tau_0)$.

When N frequency measurements $y[n]$ are available, for $n = 1, \ldots, N$, the Allan variance becomes

$$\sigma_y^2[k] = \frac{1}{2}\frac{1}{N-2k+1}\sum_{n=k}^{N-k} E\left[\left(y_k[n+k] - y_k[n]\right)^2\right] \tag{7}$$

where $k = \tau/\tau_0$ is the discrete-time observation interval, E is the ensemble average operator (expected value), and the average frequency measurements $y_k[n+k]$, $y_k[n]$ are defined as

$$y_k[n+k] = \frac{1}{k}\sum_{m=1}^{k} y[n+m] \tag{8}$$

$$y_k[n] = \frac{1}{k}\sum_{m=1}^{k} y[n-m+1] \tag{9}$$

When N is even, the maximum observation interval at which we can evaluate $\sigma_y^2[k]$ is $k = N/2$. To carry out calculations, it is useful to rewrite the Allan variance as

$$\sigma_y^2[k] = \frac{1}{2}\frac{1}{N-2k+1} \times\sum_{n=k}^{N-k}\left(E[y_k^2[n+k]] + E[y_k^2[n]] - 2E[y_k[n+k]y_k[n]]\right) \tag{10}$$

The quantity $\sigma_y^2[k]$ is a theoretical value, because infinite realizations of the random process $y[n]$ are needed to evaluate the ensemble average E. In practical applications, one typically has a single realization of the frequency measurements $y[n]$, and the Allan variance is evaluated through the estimator

$$\hat{\sigma}_y^2[k] = \frac{1}{2}\frac{1}{N-2k+1}\sum_{n=k}^{N-k}\left(y_k[n+k] - y_k[n]\right)^2 \tag{11}$$

The Allan variance can be also written with respect to time measurements. First, by using (6), the average frequency measurements (8) and (9) are rewritten as

$$y_k[n+k] = \frac{x[n+k] - x[n]}{k\tau_0} \tag{12}$$

$$y_k[n] = \frac{x[n] - x[n-k]}{k\tau_0} \tag{13}$$

Then, they are replaced in (7), obtaining

$$\sigma_y^2[k] = \frac{1}{2}\frac{1}{N-2k+1} \times\sum_{n=k}^{N-k}\frac{E\left[\left(x[n+k] - 2x[n] + x[n-k]\right)^2\right]}{k^2\tau_0^2} \tag{14}$$

The corresponding Allan variance estimator for time measurements is given by

$$\hat{\sigma}_y^2[k] = \frac{1}{2}\frac{1}{N-2k+1} \times\sum_{n=k}^{N-k}\frac{\left(x[n+k] - 2x[n] + x[n-k]\right)^2}{k^2\tau_0^2} \tag{15}$$

1) White Frequency Modulation: A WFM $y(t)$ can be modeled by a white Gaussian noise with zero mean and autocorrelation function

$$R_y(t', t'') = E[y(t')y(t'')] = \sigma^2\delta(t' - t'') \tag{16}$$

where $\delta(t)$ is a Dirac delta function. Consequently, from (5), the frequency measurements $y[n]$ are Gaussian and have mean and variance given by, respectively,

$$E[y[n]] = 0 \tag{17}$$

$$E[(y[n] - E[y[n]])^2] = E[y^2[n]] = \frac{\sigma^2}{\tau_0} \tag{18}$$

Moreover, from (5), it can be also shown that the frequency measurements are uncorrelated, namely, the autocorrelation function for $n \neq m$ is given by

$$E[y[n]y[m]] = 0 \tag{19}$$

Therefore, since the frequency measurements are Gaussian and uncorrelated, they are statistically independent.

Appendix 1 shows that the Allan deviation for WFM with full data is given by [2]

$$\sigma_y[k] = \sigma(k\tau_0)^{-1/2} \tag{20}$$

In continuous time,

$$\sigma_y(\tau) = \sigma\tau^{-1/2} \tag{21}$$

2) White Phase Modulation: A WPM can be modeled by Gaussian time measurements $x[n]$ with mean and variance given by, respectively,

$$E[x[n]] = 0 \tag{22}$$

$$E[(x[n] - E[x[n]])^2] = E[x^2[n]] = \sigma^2 \tag{23}$$

and autocorrelation function given by, for $n \neq m$,

$$E[x[n]x[m]] = 0 \tag{24}$$

Being Gaussian and uncorrelated, the time measurements are statistically independent. Consequently, from (6), also the frequency measurements are Gaussian, with mean and variance given by, respectively,

$$E[y[n]] = 0 \tag{25}$$

$$E[(y[n] - E[y[n]])^2] = E[y^2[n]] = \frac{2\sigma^2}{\tau_0^2} \tag{26}$$

and autocorrelation function given by, for $n \neq m$,

$$E[y[n]y[m]] = \begin{cases} -\frac{\sigma^2}{\tau_0^2}, & \text{for } |n-m| = 1 \\ 0, & \text{for } |n-m| > 1 \end{cases} \tag{27}$$

Appendix 2 shows that the Allan deviation for WPM is given by [2]

$$\sigma_y[k] = \sqrt{3}\sigma(k\tau_0)^{-1} \tag{28}$$

In continuous time

$$\sigma_y(\tau) = \sqrt{3}\sigma\tau^{-1} \tag{29}$$

3) Random Walk Frequency Modulation: An RWFM can be modeled by a normalized frequency deviation defined as

$$y(t) = \int_0^t \xi(t')dt' \tag{30}$$

where $\xi(t)$ is a white Gaussian noise with mean value and autocorrelation function given by, respectively,

$$E[\xi(t)] = 0 \tag{31}$$

$$E[\xi(t')\xi(t'')] = \sigma^2\delta(t' - t'') \tag{32}$$

By using (5), the corresponding frequency measurement $y[n]$ is Gaussian, with mean value and variance given by, respectively,

$$E[y[n]] = 0 \tag{33}$$

$$E[(y[n] - E[y[n]])^2] = E[y^2[n]] = \sigma^2\tau_0\left(n - \frac{2}{3}\right) \tag{34}$$

and autocorrelation function given by, for $n \neq m$,

$$E[y[n]y[m]] = \sigma^2\tau_0\left(\min(n,m) - \frac{1}{2}\right) \tag{35}$$

The function $\min(n, m)$ returns the minimum between n and m. Appendix 3 shows the derivation of (34) and (35).

Appendix 3 also proves that the Allan deviation for RWFM is [2]

$$\sigma_y[k] = \frac{\sigma}{\sqrt{3}}(k\tau_0)^{1/2} \tag{36}$$

In continuous time,

$$\sigma_y(\tau) = \frac{\sigma}{\sqrt{3}}\tau^{1/2} \tag{37}$$

B. Missing data

Suppose now that some of the frequency measurements $y[1], \ldots, y[N]$ are missing, as happens, for example, in Fig. 1. As explained at the beginning of Sect. IV-A, the time series used to generate this picture is made by 3 samples of WFM, then 51 missing samples, another 3 samples of WFM, then 51 missing samples, and so on. If the corresponding Allan variance is estimated by considering the average frequency deviations $y_k[n+k]$ and $y_k[n]$ obtained only when all of the required frequency measurements in (8)-(9) are available, then the Allan variance could be estimated for $k = 1$ only, a basically useless result for stability analysis. To estimate the Allan deviation at any k value, we replace $y_k[n+k]$ and $y_k[n]$ in (8)-(9) with the average frequency deviations $y'_k[n+k]$ and $y'_k[n]$, obtained even if some of the required frequency measurements are missing,

$$y'_k[n+k] = \frac{1}{\#I_1(n,k)} \sum_{m \in I_1(n,k)} y[n+m] \tag{38}$$

$$y'_k[n] = \frac{1}{\#I_2(n,k)} \sum_{m \in I_2(n,k)} y[n-m+1] \tag{39}$$

where $I_1(n,k)$ is the set of discrete time instants at which $y[n+m]$ is available, for a given n and k, and $\#I_1(n,k)$ is its number of elements. The set $I_2(n,k)$ is defined accordingly. Specifically, if I_y represents the set of discrete-time values

at which the frequency measurements $y[n]$ are available, then $I_1(n,k)$ and $I_2(n,k)$ are defined as

$$I_1(n,k) = \{n+1, ..., n+k\} \cap I_y \tag{40}$$
$$I_2(n,k) = \{n-k+1, ...n\} \cap I_y \tag{41}$$

where $\cap$ is the set intersection. Consequently, the Allan variance becomes

$$\sigma_y^2[k] = \frac{1}{2}\frac{1}{\#I(k)} \sum_{n \in I(k)} E\left[\left(y_k'[n+k] - y_k'[n]\right)^2\right] \tag{42}$$

where $I(k)$ is the set of time instants n at which both $y_k'[n+k]$ and $y_k'[n]$ are available for a given k. Similarly, the Allan variance estimator becomes

$$\hat{\sigma}_y^2[k] = \frac{1}{2}\frac{1}{\#I(k)} \sum_{n \in I(k)} \left(y_k'[n+k] - y_k'[n]\right)^2 \tag{43}$$

Clearly, at those values of k for which $y_k'[n+k]$ and $y_k'[n]$ are both unavailable, the corresponding Allan variance value cannot be computed. Note that when all of the measurements are available, it is $I_y = \{1, \ldots, N\}$, $I_1(n) = \{n+1, \ldots, n+k\}$, $I_2(n) = \{n-k+1, \ldots, n\}$, $I_3(k) = \{k, \ldots, N-k\}$, and, therefore, $\#I_y = N$, $\#I_1(n,k) = \#I_2(n,k) = k$, $\#I(k) = N-2k+1$, and the Allan variance for missing data (42) equals the Allan variance for full data (7).

III. The Corrected Allan Variance

As shown by Fig. 1, it is, in general,

$$\sigma_y^2[k] \text{ (Full data)} \neq \sigma_y^2[k] \text{ (Missing data)} \tag{44}$$

where the Allan variance for full data and missing data are defined in (7) and (42), respectively. This bias is due to the fact that the terms $y_k'[n+k]$, $y_k'[n]$ in (38)-(39) are averaged over the available frequency measurements only, whereas the terms $y_k[n+k]$, $y_k[n]$ in (8)-(9) are averaged over the full set of frequency measurements.

To eliminate this bias, we propose the corrected Allan variance

$$\sigma_y^2[k] = \frac{1}{2}\frac{1}{\#I(k)} \sum_{n \in I(k)} \alpha^2(n,k) E\left[\left(y_k'[n+k] - y_k'[n]\right)^2\right] \tag{45}$$

where $\alpha^2(n,k)$ is a correction factor given by

$$\alpha^2(n,k) = \frac{E\left[\left(y_k[n+k] - y_k[n]\right)^2\right]}{E\left[\left(y_k'[n+k] - y_k'[n]\right)^2\right]} \tag{46}$$

With this correction, it is immediate to see that

$$\sigma_y^2[k] \text{ (Corrected)} = \sigma_y^2[k] \text{ (Full data)} \tag{47}$$

This equality holds at those k values where the corrected Allan variance exists. Consequently, the corrected Allan variance estimator is defined as

$$\hat{\sigma}_y^2[k] = \frac{1}{2}\frac{1}{\#I(k)} \sum_{n \in I(k)} \alpha^2(n,k) \left(y_k'[n+k] - y_k'[n]\right)^2 \tag{48}$$

The matrix technique discussed in the next section simplifies the calculation of the correction factor.

Note that all of the figures in the examples have been obtained by directly implementing the corrected Allan variance estimator defined in (48), through the matrix calculus technique described in Sect. III-A. This algorithm is far from being optimal. A fast algorithm can be obtained by improving this algorithm in several ways. For example, when many data are missing, one can take advantage of the sparsity of the vector $I(k)$ in (48). To give an estimate of the computational cost required to generate the displayed figures, two facts can be considered. First, that for all of the figures in the paper, the corrected Allan variance estimator is approximately 1.1-10.5 times slower than the Allan variance estimator without correction, depending on the figure. Second, more importantly, that any estimate of the corrected Allan variance shown in the paper required a computational time < 25 s on a commercial desktop computer, with 1.9 s being the fastest estimate.

A. Correction Factor: Matrix Calculus Technique

The correction factor $\alpha^2(n,k)$ can be obtained from the expanded form

$$\alpha^2(n,k) = \frac{E\left[\left(y_k[n+k] - y_k[n]\right)^2\right]}{E[y_k'^2[n+k]] + E[y_k'^2[n]] - 2E[y_k'[n+k]y_k'[n]]} \tag{49}$$

For WFM, WPM, and RWFM, the numerator is derived in Appendices 1-3, whereas the terms $E[y_k'^2[n+k]]$, $E[y_k'^2[n]]$, and $E[y_k'[n+k]y_k'[n]]$ at the denominator can be computed by introducing a matrix notation. Specifically,

$$E[y_k'^2[n+k]] = \frac{1}{\#I_1^2(k)} \sum_{i \in I_1(k)} \sum_{j \in I_1(k)} \boldsymbol{A}[i,j] \tag{50}$$

$$E[y_k'^2[n]] = \frac{1}{\#I_2^2(k)} \sum_{i \in I_2(k)} \sum_{j \in I_2(k)} \boldsymbol{B}[i,j] \tag{51}$$

$$E[y_k'[n+k]y_k'[n]] = \frac{1}{\#I_1(k)\#I_2(k)} \sum_{i \in I_1(k)} \sum_{j \in I_2(k)} \boldsymbol{C}[i,j] \tag{52}$$

where the k-by-k matrices $\boldsymbol{A}$, $\boldsymbol{B}$, and $\boldsymbol{C}$ are defined as

$$\boldsymbol{A} = E[\boldsymbol{y}_k'[n+k]\boldsymbol{y}_k'[n+k]^T] \tag{53}$$
$$\boldsymbol{B} = E[\boldsymbol{y}_k'[n]\boldsymbol{y}_k'[n]^T] \tag{54}$$
$$\boldsymbol{C} = E[\boldsymbol{y}_k'[n+k]\boldsymbol{y}_k'[n]^T] \tag{55}$$

and the k-by-1 vectors $\boldsymbol{y}_k'[n+k]$, $\boldsymbol{y}_k'[n]$ are given by

$$\boldsymbol{y}_k'[n+k] = \begin{bmatrix} y[n+1] \\ \vdots \\ y[n+k] \end{bmatrix}, \quad \boldsymbol{y}_k'[n] = \begin{bmatrix} y[n-k+1] \\ \vdots \\ y[n] \end{bmatrix} \tag{56}$$

The notation $\boldsymbol{y}_k'[n+k]^T$ indicates the transpose of $\boldsymbol{y}_k'[n+k]$. The matrices $\boldsymbol{A}$, $\boldsymbol{B}$, and $\boldsymbol{C}$ can be computed for WFM, WPM, and RWFM by using the corresponding variances and autocorrelation functions given in Sects. II-A1-II-A3, as shown in the subsequent sections.

B. Correction Factor: White Frequency Modulation

The correction factor for WFM is given by

$$\alpha^2_{\text{WFM}}(n,k) = \frac{2k^{-1}}{\frac{1}{\#I_1(k)} + \frac{1}{\#I_2(k)}} \tag{57}$$

This result is obtained by first using (99) for the numerator of (49). Then, for the denominator of (49), one notes that

$$\boldsymbol{A}_{\text{WFM}} = \boldsymbol{B}_{\text{WFM}} = \frac{\sigma^2}{\tau_0}\boldsymbol{I} \tag{58}$$

$$\boldsymbol{C}_{\text{WFM}} = 0 \tag{59}$$

where $\boldsymbol{I}$ is the k-by-k identity matrix. The terms on the main diagonal of the matrices $\boldsymbol{A}_{\text{WFM}}$ and $\boldsymbol{B}_{\text{WFM}}$ are obtained by using the variance (18), whereas the off-diagonal terms and the matrix $\boldsymbol{C}_{\text{WFM}}$ are obtained from the autocorrelation function (19). By substituting these results in (50)-(52), it is

$$E[y'^2_k[n+k]] = \frac{1}{\#I_1(k)}\frac{\sigma^2}{\tau_0} \tag{60}$$

$$E[y'^2_k[n]] = \frac{1}{\#I_2(k)}\frac{\sigma^2}{\tau_0} \tag{61}$$

$$E[y'_k[n+k]y'_k[n]] = 0 \tag{62}$$

As an example, the derivation of (60) is

$$E[y'^2_k[n+k]] = \frac{1}{\#I_1^2(k)} \sum_{i\in I_1(k)} \sum_{j\in I_1(k)} \boldsymbol{A}_{\text{WFM}}[i,j] \tag{63}$$

$$= \frac{1}{\#I_1^2(k)}\frac{\sigma^2}{\tau_0} \sum_{i\in I_1(k)} \boldsymbol{I} \tag{64}$$

$$= \frac{1}{\#I_1^2(k)}\frac{\sigma^2}{\tau_0} \#I_1(k) \tag{65}$$

$$= \frac{1}{\#I_1(k)}\frac{\sigma^2}{\tau_0} \tag{66}$$

The same procedure is used for $E[y'^2_k[n]]$ and $E[y'_k[n+k]y'_k[n]]$.

C. Correction Factor: White Phase Modulation

The correction factor for WPM is given by

$$\alpha^2_{\text{WPM}}(n,k) = 6k^{-2}\left[\frac{1}{\#I_1^2(k)} \sum_{i\in I_1(k)} \sum_{j\in I_1(k)} \boldsymbol{A}'_{\text{WPM}}[i,j]\right. \tag{67}$$

$$+ \frac{1}{\#I_2^2(k)} \sum_{i\in I_2(k)} \sum_{j\in I_2(k)} \boldsymbol{B}'_{\text{WPM}}[i,j] \tag{68}$$

$$\left. -2\frac{1}{\#I_1(k)\#I_2(k)} \sum_{i\in I_1(k)} \sum_{j\in I_2(k)} \boldsymbol{C}'_{\text{WPM}}[i,j]\right]^{-1} \tag{69}$$

where

$$\boldsymbol{A}'_{\text{WPM}} = \boldsymbol{B}'_{\text{WPM}} = \begin{bmatrix} 2 & -1 & 0 & \cdots & 0 \\ -1 & 2 & -1 & \ddots & \vdots \\ 0 & -1 & \ddots & \ddots & 0 \\ \vdots & \ddots & \ddots & \ddots & -1 \\ 0 & \cdots & 0 & -1 & 2 \end{bmatrix} \tag{70}$$

$$\boldsymbol{C}'_{\text{WPM}} = \begin{bmatrix} 0 & \cdots & 0 & -1 \\ \vdots & \ddots & \ddots & 0 \\ \vdots & \ddots & \ddots & \vdots \\ 0 & \cdots & \cdots & 0 \end{bmatrix} \tag{71}$$

To obtain this result, one first uses (106) for the numerator of (49), whereas, for the denominator, it is

$$\boldsymbol{A}_{\text{WPM}} = \boldsymbol{B}_{\text{WPM}} = \frac{\sigma^2}{\tau_0^2}\boldsymbol{A}'_{\text{WPM}} \tag{72}$$

$$\boldsymbol{C}_{\text{WPM}} = \frac{\sigma^2}{\tau_0^2}\boldsymbol{C}'_{\text{WPM}} \tag{73}$$

The terms on the main diagonal of the symmetric tridiagonal matrices $\boldsymbol{A}_{\text{WPM}}$ and $\boldsymbol{B}_{\text{WPM}}$ are obtained by using the variance (26), whereas the off-diagonal terms and the matrix $\boldsymbol{C}_{\text{WPM}}$ are derived from the autocorrelation function (27).

D. Correction Factor: Random Walk Frequency Modulation

The correction factor for RWFM is given by

$$\alpha^2_{\text{RWFM}}(n,k) = \frac{2}{3}k\left[\frac{1}{\#I_1^2(k)} \sum_{i\in I_1(k)} \sum_{j\in I_1(k)} \boldsymbol{A}'_{\text{RWFM}}[i,j]\right. \tag{74}$$

$$+ \frac{1}{\#I_2^2(k)} \sum_{i\in I_2(k)} \sum_{j\in I_2(k)} \boldsymbol{B}'_{\text{RWFM}}[i,j] \tag{75}$$

$$\left. -2\frac{1}{\#I_1(k)\#I_2(k)} \sum_{i\in I_1(k)} \sum_{j\in I_2(k)} \boldsymbol{C}'_{\text{RWFM}}[i,j]\right]^{-1} \tag{76}$$

where

$$\boldsymbol{A}'_{\text{RWFM}} = \begin{bmatrix} n+\frac{1}{3} & n+\frac{1}{2} & \cdots & n+\frac{1}{2} & n+\frac{1}{2} \\ n+\frac{1}{2} & n+\frac{4}{3} & \cdots & n+\frac{3}{2} & n+\frac{3}{2} \\ \vdots & \vdots & \ddots & \vdots & \vdots \\ n+\frac{1}{2} & n+\frac{3}{2} & \cdots & n+k-\frac{5}{3} & n+k-\frac{3}{2} \\ n+\frac{1}{2} & n+\frac{3}{2} & \cdots & n+k-\frac{3}{2} & n+k-\frac{2}{3} \end{bmatrix} \tag{77}$$

$$\boldsymbol{B}'_{\text{RWFM}} = \begin{bmatrix} n-k+\frac{1}{3} & n-k+\frac{1}{2} & \cdots & n-k+\frac{1}{2} & n-k+\frac{1}{2} \\ n-k+\frac{1}{2} & n-k+\frac{4}{3} & \cdots & n-k+\frac{3}{2} & n-k+\frac{3}{2} \\ \vdots & \vdots & \ddots & \vdots & \vdots \\ n-k+\frac{1}{2} & n-k+\frac{3}{2} & \cdots & n-\frac{5}{3} & n-\frac{3}{2} \\ n-k+\frac{1}{2} & n-k+\frac{3}{2} & \cdots & n-\frac{3}{2} & n-\frac{2}{3} \end{bmatrix} \tag{78}$$

$$\boldsymbol{C}'_{\text{RWFM}} = \begin{bmatrix} n-k+\frac{1}{2} & n-k+\frac{3}{2} & \cdots & n-\frac{3}{2} & n-\frac{1}{2} \\ n-k+\frac{1}{2} & n-k+\frac{3}{2} & \cdots & n-\frac{3}{2} & n-\frac{1}{2} \\ \vdots & \vdots & \ddots & \vdots & \vdots \\ n-k+\frac{1}{2} & n-k+\frac{3}{2} & \cdots & n-\frac{3}{2} & n-\frac{1}{2} \\ n-k+\frac{1}{2} & n-k+\frac{3}{2} & \cdots & n-\frac{3}{2} & n-\frac{1}{2} \end{bmatrix} \tag{79}$$

This result is obtained by first using (135) for the numerator of (49), whereas, for the denominator, it is

$$\boldsymbol{A}_{\text{RWFM}} = \sigma^2\tau_0\boldsymbol{A}'_{\text{RWFM}} \tag{80}$$
$$\boldsymbol{B}_{\text{RWFM}} = \sigma^2\tau_0\boldsymbol{B}'_{\text{RWFM}} \tag{81}$$
$$\boldsymbol{C}_{\text{RWFM}} = \sigma^2\tau_0\boldsymbol{C}'_{\text{RWFM}} \tag{82}$$

The terms on the main diagonals of the matrices $\boldsymbol{A}_{\text{RWFM}}$ and $\boldsymbol{B}_{\text{RWFM}}$ are derived from the variance (34), whereas the off-diagonal terms and the matrix $\boldsymbol{C}_{\text{RWFM}}$ are obtained by using the autocorrelation function (35).

E. Multiple Noise Components

Suppose that the normalized frequency deviation of a clock is made by the sum of two statistically independent noise components, such as, for instance, WFM and WPM,

$$y(t) = y_{\text{WFM}}(t) + y_{\text{WPM}}(t) \tag{83}$$

Then, when all of the frequency measurements are available, it is

$$\sigma_y^2[k]\ \text{(Full data)} = \sigma_{y,\text{WFM}}^2[k]\ \text{(Full data)} + \sigma_{y,\text{WPM}}^2[k]\ \text{(Full data)} \tag{84}$$

Appendix 5 shows how to derive this classical result. When data are missing, for a given set of observation interval values the correction can be computed for one noise component only, therefore,

$$\sigma_y^2[k]\ \text{(Corrected)} \neq \sigma_y^2[k]\ \text{(Full data)} \tag{85}$$

As Appendix 6 in fact shows, for a WFM correction, it is

$$\sigma_y^2[k]\ \text{(Corrected)} = \sigma_{y,\text{WFM}}^2[k]\ \text{(Full data)} + \sigma_{y,\text{WPM}}^2[k]\ \text{(Corrected for WFM)} \tag{86}$$

However, if WFM is a dominant noise component in a given region of the observation interval, namely,

$$\sigma_{y,\text{WFM}}^2[k]\ \text{(Full data)} \gg \sigma_{y,\text{WPM}}^2[k]\ \text{(Full data)} \tag{87}$$

then

$$\sigma_y^2[k]\ \text{(Full data)} \approx \sigma_{y,\text{WFM}}^2[k]\ \text{(Full data)} \tag{88}$$

and the numerical simulations show that this result holds also for the corrected Allan variance, namely,

$$\sigma_y^2[k]\ \text{(Corrected)} \approx \sigma_y^2[k]\ \text{(Full data)} \tag{89}$$

where the correction is computed for WFM. This approximation should be derived analytically, but the proof is difficult because it must be obtained for any pattern of missing data I_y. Anyway, Monte Carlo simulations, such as those presented in Sect. IV-B, show that this approximation is effective. In general, clock specifications establish the dominant noise component in every observation interval region.

IV. Examples

The corrected Allan variance and its estimator are now validated through Monte Carlo simulations first for WFM, WPM, and RWFM components individually, and then for multiple noise components. The problem of choosing wrong noise components is also discussed.

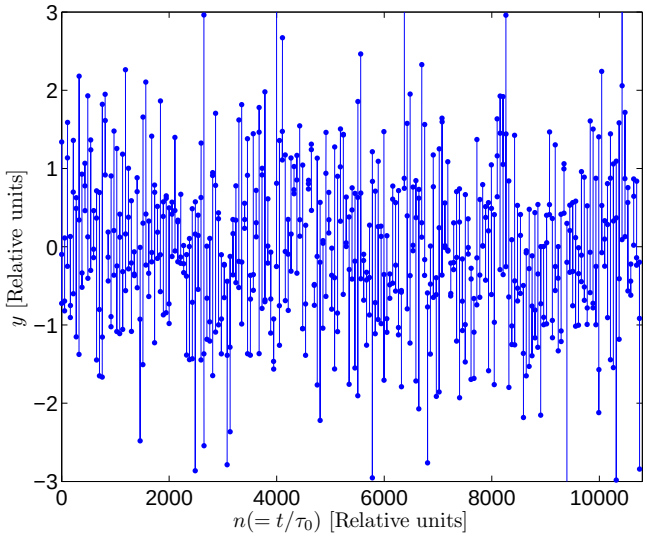

Fig. 2. Simulated frequency measurements for WFM with blocks of missing data. The time series is made by 3 WFM data, then 51 missing data, another 3 WFM data, then 51 missing data, and so on. (The pattern of missing data is described in detail at the beginning of Sect. IV-A.) The first 1000 samples of the time series can be seen in Fig. 3.

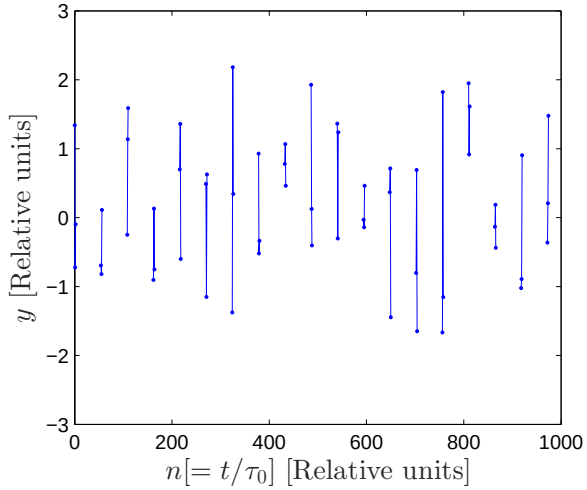

Fig. 3. The first 1000 samples of the WFM shown in Fig. 2. The missing data blocks can be clearly seen.

A. Individual Noise Components

A time series with $N = 10800$ samples, made of 200 blocks with 54 samples each, is simulated. Each block has 3 data and then 51 missing data. The percentage of missing data is therefore $51/54 \times 100 \approx 94\%$. The case of uniformly distributed missing data is also considered for WFM and WPM. A time series with $N = 10800$ data is simulated, and then 94% of the data are randomly removed by selecting their discrete-time instants from a uniform distribution.

1) White Frequency Modulation: Figure 2 shows the simulated frequency measurements $y[n]$ for a WFM with blocks of missing data. To better illustrate the structure of the missing data blocks, the first 1000 samples are shown in Fig. 3. The corresponding stability analysis is given in Fig. 4. The

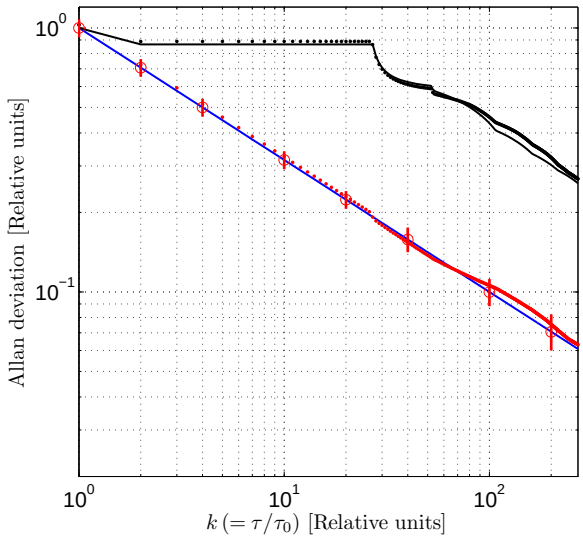

Fig. 4. Stability analysis for the WFM with blocks of missing data of Fig. 2. The blue curve is the Allan deviation for the full data case, whereas the black curve is the Allan deviation for the missing data case without correction. The estimated Allan deviation for missing data without correction is represented by the dotted black curve. The red circles represent the corrected Allan deviation, whereas the dotted red curve is the estimate of the corrected Allan deviation. The red bars are 95% confidence intervals for the corrected Allan deviation estimator.

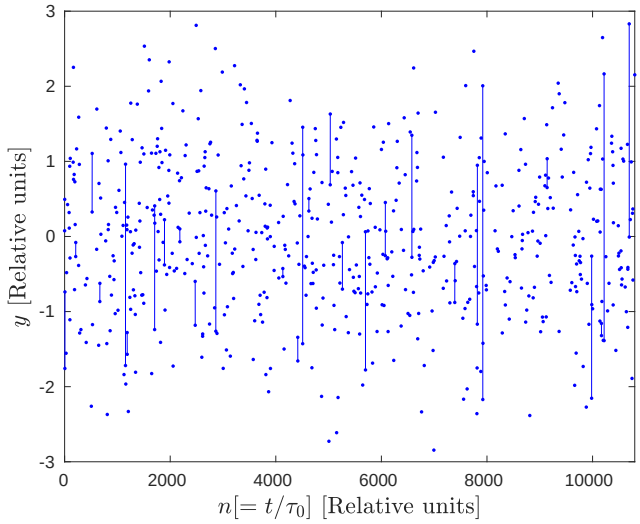

Fig. 5. Simulated frequency measurements for WFM with uniformly distributed missing data. This pattern of missing data is described in detail at the beginning of Sect. IV-A.

blue line represents the theoretical Allan deviation for full data, which exhibits the expected $\tau^{-1/2}$ behavior ($k^{-1/2}$ in discrete-time). The solid black line represents the theoretical Allan deviation for missing data. This curve is dramatically different from the expected behavior. It is in fact flat for small observation intervals, and then it decreases with a slope similar to the $\tau^{-1/2}$ behavior. The black dotted curve is the estimated Allan deviation for missing data without the correction, and, as expected, it is consistent with the theoretical Allan deviation for missing data. The red dotted curve is the estimated Allan deviation for missing data with the correction, and it follows the expected theoretical behavior. The red circles represent

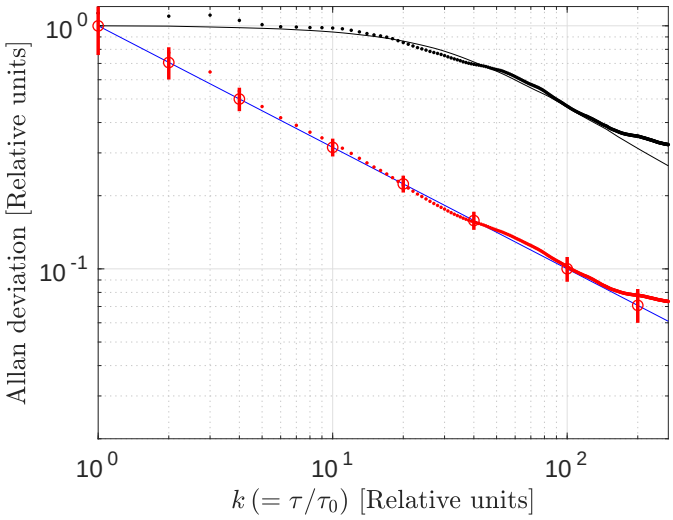

Fig. 6. Stability analysis for the WFM with uniformly distributed missing data of Fig. 5. The blue curve is the Allan deviation for the full data case, whereas the black curve is the Allan deviation for the missing data case without correction. The estimated Allan deviation for missing data without correction is represented by the dotted black curve. The red circles represent the corrected Allan deviation, whereas the dotted red curve is the estimate of the corrected Allan deviation. The red bars are 95% confidence intervals for the corrected Allan deviation estimator.

the corrected Allan deviation, obtained through Monte Carlo simulations. The red circles are located on the theoretical Allan deviation for full data, and this result validates the calculations of the corrected Allan deviation for the WFM case. Finally, the red bars are 95% confidence intervals obtained through Monte Carlo simulations.

Figure 5 instead shows the simulated frequency measurements for uniformly distributed missing data. The corresponding stability analysis is given in Fig. 6. The Allan deviation for missing data (solid black curve) exhibits again a flat behavior for small observation intervals, and then it follows the expected $\tau^{-1/2}$ behavior (blue curve). The estimated Allan deviation with the correction (red dotted curve) follows the expected behavior for full data.

2) White Phase Modulation: The simulated frequency measurements for a WPM with blocks of missing data are given in Fig. 7. Figure 8 shows instead the corresponding stability analysis. The Allan deviation for missing data (solid black curve) does not follow the expected τ^{-1} behavior represented by the Allan deviation for full data (blue curve), because it is flat for small observation interval values, and then it decreases with a slope that does not correspond to τ^{-1}. The estimated Allan deviation for missing data with the correction (red dotted line) follows the expected behavior, and the confidence intervals (red bars) are smaller than in the WFM case. The corrected Allan deviation (red circles), obtained through Monte Carlo simulations, follows the Allan deviation for full data, therefore validating the correction for WPM.

The simulated frequency measurements for the case of uniformly distributed missing data are shown in Fig. 9, and the corresponding stability analysis is represented in Fig. 10. Surprisingly, the Allan deviation for missing data (solid black curve), shows a $\tau^{-1/2}$ behavior, corresponding to WFM, rather

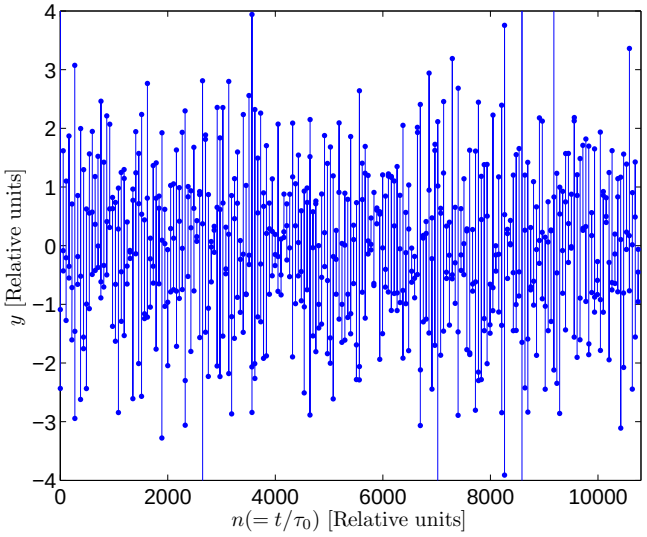

Fig. 7. Simulated frequency measurements for WPM with blocks of missing data. This pattern of missing data is described in detail at the beginning of Sect. IV-A.

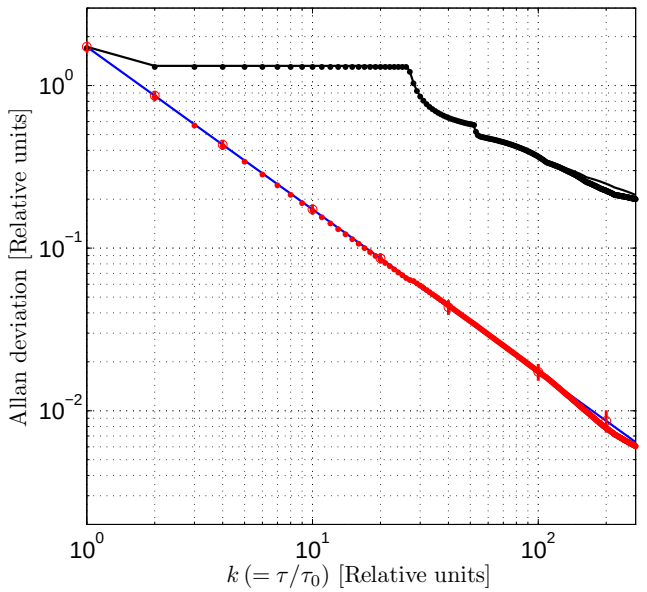

Fig. 8. Stability analysis for the WPM with blocks of missing data of Fig. 7. The blue curve is the Allan deviation for the full data case, whereas the black curve is the Allan deviation for the missing data case without correction. The estimated Allan deviation for missing data without correction is represented by the dotted black curve. The red circles represent the corrected Allan deviation, whereas the dotted red curve is the estimate of the corrected Allan deviation. The red bars are 95% confidence intervals for the corrected Allan deviation estimator.

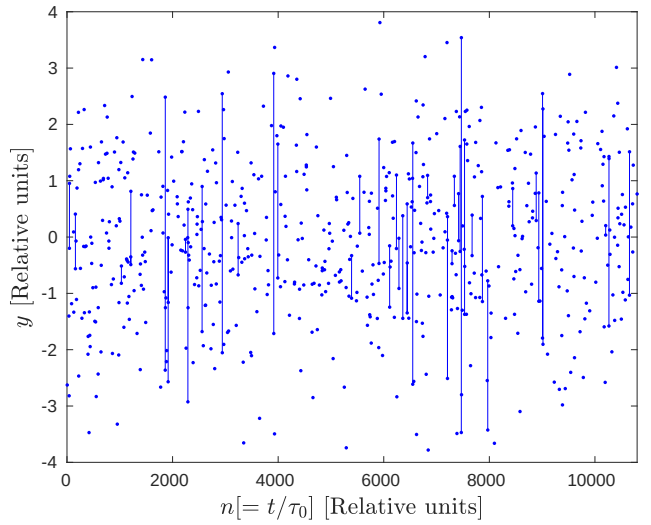

Fig. 9. Simulated frequency measurements for WPM with uniformly distributed missing data. This pattern of missing data is described in detail at the beginning of Sect. IV-A.

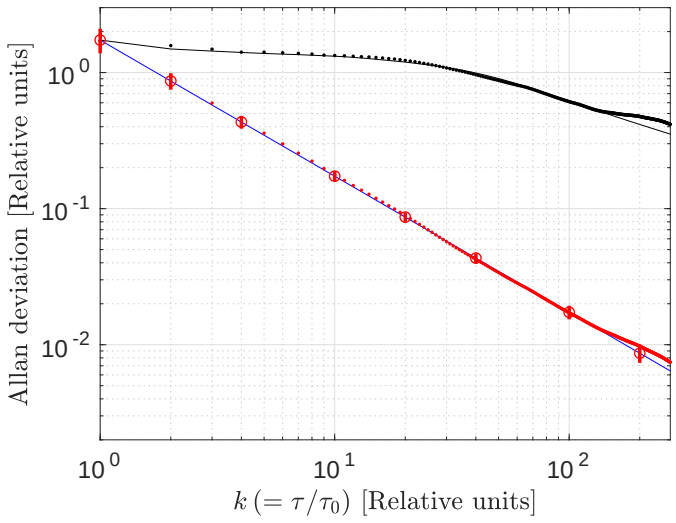

Fig. 10. Stability analysis for the WPM with uniformly distributed missing data of Fig. 9. The blue curve is the Allan deviation for the full data case, whereas the black curve is the Allan deviation for the missing data case without correction. The estimated Allan deviation for missing data without correction is represented by the dotted black curve. The red circles represent the corrected Allan deviation, whereas the dotted red curve is the estimate of the corrected Allan deviation. The red bars are 95% confidence intervals for the corrected Allan deviation estimator.

than WPM. This discrepancy is eliminated by the corrected Allan deviation (red circles), along with its estimate (dotted red curve).

3) Random Walk Frequency Modulation: The simulated frequency measurements for RWFM in the case of blocks of missing data are shown in Fig. 11. The corresponding stability analysis is represented in Fig. 12. The Allan deviation for full data (blue curve) has the typical $\tau^{1/2}$ behavior. The Allan deviation for missing data (solid black curve) does not follow this expected behavior, but it is flat for small and medium observation interval values, and it gets closer to the blue curve only for large observation interval values. The corrected

Allan deviation (red circles) eliminates this divergence, and its estimate (red dotted curve) follows the $\tau^{1/2}$ behavior. The confidence intervals (red bars) are larger than for the WFM and WPM cases.

B. Multiple Noise Components

First, similarly to the case of individual noise components of Sect. IV-A, a time series with $N = 10800$ samples, made of 200 blocks with 54 samples each, is simulated. Each block has now 15 data and then 39 missing data, resulting in approximately 72% of missing data. For WPM-WFM, the case of blocks of missing data with fixed length but random position is also considered.

1) WPM-WFM: Figure 13 shows the simulated frequency measurements in case of blocks of missing data for the sum of a WPM and a WFM. The corresponding stability analysis is represented in Fig. 14. The Allan deviation of the individual WPM and WFM components is represented by the dashed blue lines, with slopes τ^{-1} (k^{-1} in discrete time) and $\tau^{-1/2}$ ($k^{-1/2}$ in discrete time), respectively. From (84), for the case of full data, the Allan deviation of the sum of WPM and WFM (solid blue line) is given by

$$\sigma_y[k] \text{ (Full data)} = \sqrt{\sigma^2_{y,\text{WPM}}[k] \text{ (Full data)} + \sigma^2_{y,\text{WFM}}[k] \text{ (Full data)}} \tag{90}$$

The black circles indicate the Allan deviation for missing data without correction, and the red circles indicate the corrected Allan deviation. The estimated Allan deviation without correction is indicated by the black dots, and the estimate of the corrected Allan deviation by the red dots. The correction is for WPM at small observation interval values, and for WFM at large interval values, where these noise components are dominant. In the transition region, located in the intermediate observation interval region, the correction is not computed because a dominant noise component does not exist. In the WPM region the corrected Allan deviation completely removes the bias. In the WFM region the corrected Allan deviation largely reduces the bias, and only a residual bias remains, as predicted in Sect. III-E. The red bars are 95% confidence intervals.

Figure 15 shows the first 1000 samples of the frequency deviation for the sum of WPM and WFM when random blocks of missing data are considered. As in the previous case, the time series as $N = 10800$ samples, and it is made by 200 blocks with 54 samples, with 15 data and 39 missing data each. The position of the sub-block with the 15 data is now randomly distributed within each block. The corresponding stability analysis is shown in Fig. 16. This picture is basically identical to Fig. 14, the only difference being that the Allan deviation without correction shows a larger bias for $k = 60$. The picture is a further proof that the proposed method can work with any pattern of missing data.

2) WPM-RWFM: Figure 17 shows the frequency deviation for the sum of a WPM and an RWFM noise components with the fixed blocks of missing data described at the beginning of Sect. IV-B. The corresponding stability analysis is shown in Fig. 18. The dashed blue lines with slopes τ^{-1} (k^{-1} in

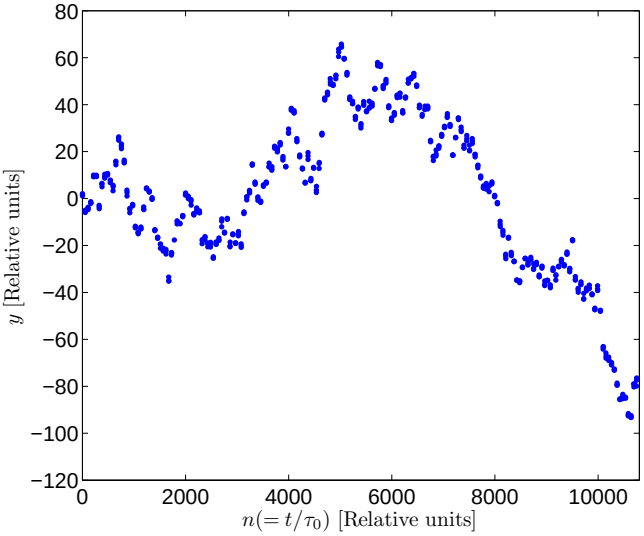

Fig. 11. Simulated frequency measurements for RWFM with blocks of missing data. This pattern of missing data is described in detail at the beginning of Sect. IV-B.

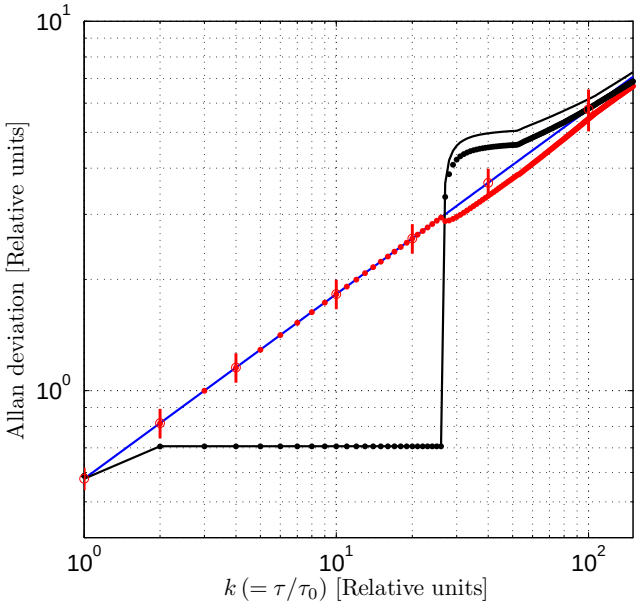

Fig. 12. Stability analysis for the RWFM with blocks of missing data of Fig. 11. The blue curve is the Allan deviation for the full data case, whereas the black curve is the Allan deviation for the missing data case. The estimated Allan deviation for missing data without correction is represented by the dotted black curve. The red circles represent the corrected Allan deviation, whereas the dotted red curve is the estimate of the corrected Allan deviation. The red bars are 95% confidence intervals for the corrected Allan deviation estimator.

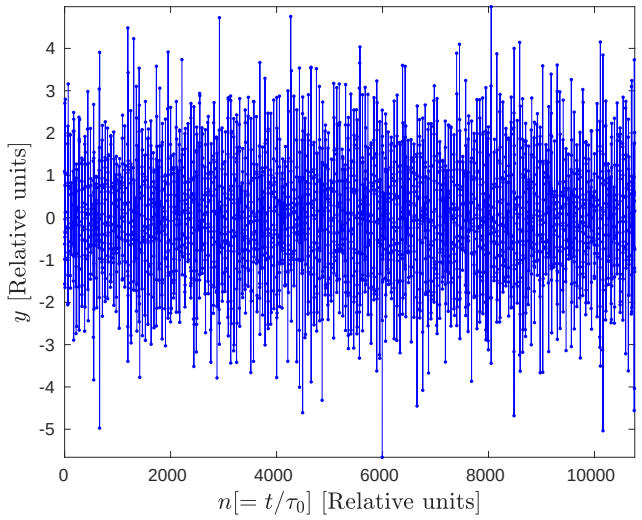

Fig. 13. Simulated frequency measurements for the sum of a WPM and a WFM with blocks of missing data. The time series is made by 15 WPM+WFM data, then 39 missing data, another 15 WPM+WFM data, then 39 missing data, and so on. (Figure 3 illustrates this pattern of missing data for WFM.) This pattern of missing data is described in detail at the beginning of Sect. IV-B.

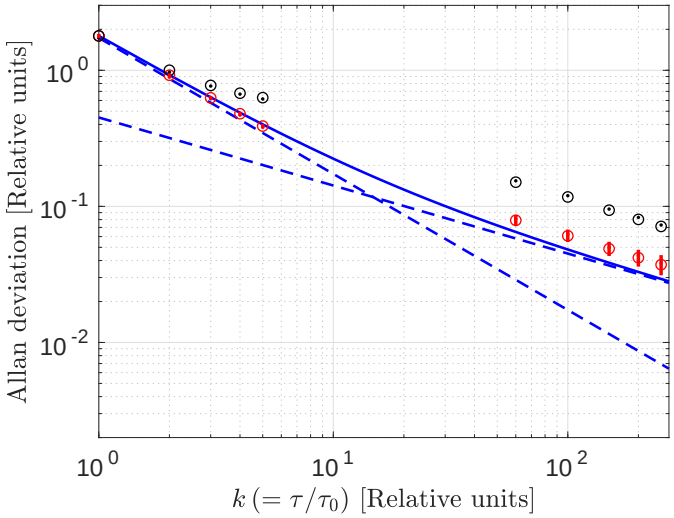

Fig. 14. Stability analysis for the sum of WPM and WFM with blocks of missing data shown in Fig. 13. The dashed blue curves with slopes τ^{-1} and $\tau^{-1/2}$ (k^{-1} and $k^{-1/2}$ in discrete time) are the Allan deviations for the individual WPM and WFM components, respectively, in the full data case, whereas the solid blue curve is the Allan deviation for the sum of the two noise components, obtained through (90). The black circles indicate the Allan deviation for the missing data case. The estimated Allan deviation in the missing data case without correction is represented by the dotted black curve. The red circles represent the corrected Allan deviation. The red bars are 95% confidence intervals for the corrected Allan deviation estimator. The corrected Allan deviation completely removes the bias for WPM, and largely reduces the bias for WFM.

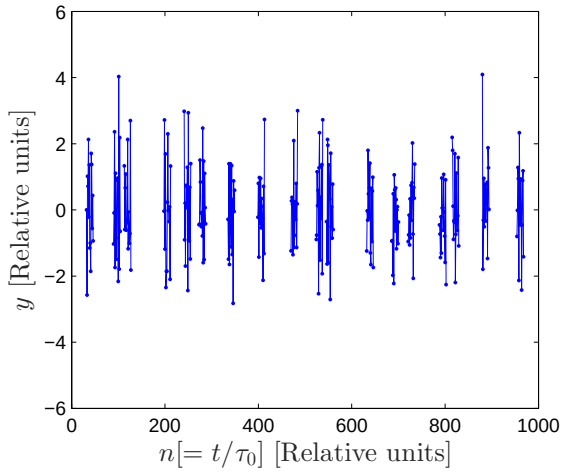

Fig. 15. Simulated frequency measurements for the sum of a WPM and a WFM with random blocks of missing data. The plot shows the first 1000 samples of a WPM+WFM noise. Within each of the 200 blocks made of 54 samples each, the position of the 15 WPM+WFM data is chosen randomly. This pattern of missing data is described in detail at the beginning of Sect. IV-B.

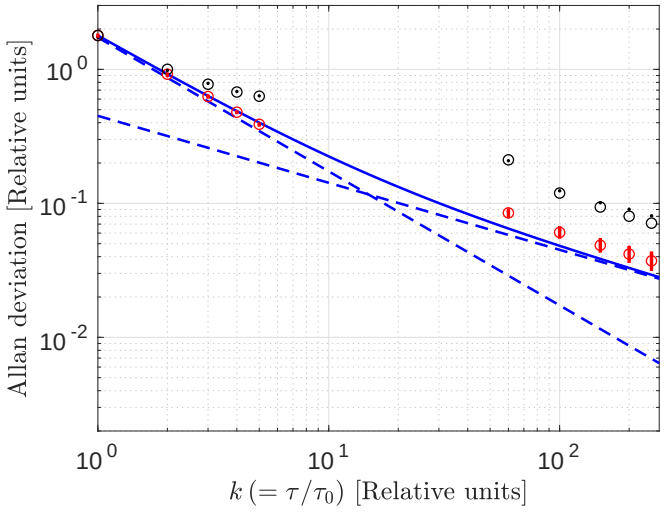

Fig. 16. Stability analysis for the sum of WPM and WFM with random blocks of missing data shown in Fig. 15. As in Fig. 14, the corrected Allan deviation (red circles) completely removes the bias for WPM, and largely reduces the bias for WFM. The only difference is that, for $k = 60$, the Allan deviation without correction (black circles) shows a larger bias with respect to Fig. 14.

discrete time) and $\tau^{1/2}$ ($k^{1/2}$ in discrete time) represent the Allan deviations for WPM and RWFM, respectively, when all of the data are available. The solid blue line is their sum, obtained through (90). The black circles represent the Allan deviation for missing data without correction, the red circles the corrected Allan deviation for missing data. The black and red dots represent estimates of the Allan deviation for missing data without correction, and of the corrected Allan deviation, respectively. The red bars are 95% confidence intervals. The correction is computed for WPM for small observation interval values, where WPM dominates, and for RWFM for large observation interval values, where RWFM dominates. As in Fig. 14, the correction is not computed in the intermediate

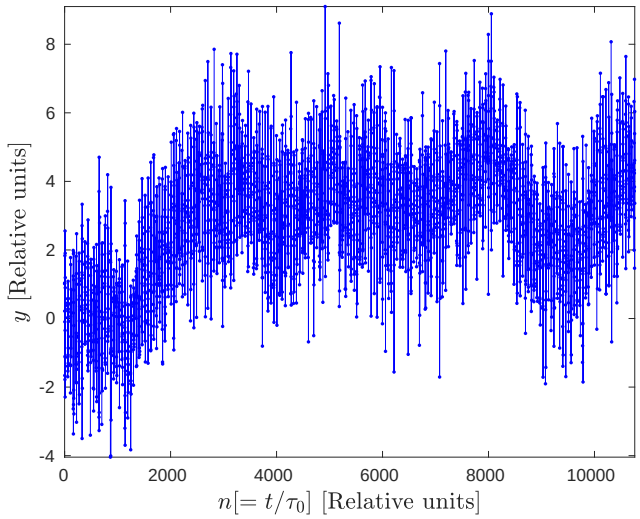

Fig. 17. Simulated frequency measurements for the sum of WPM and RWFM with blocks of missing data. This pattern of missing data is described in detail at the beginning of Sect. IV-B.

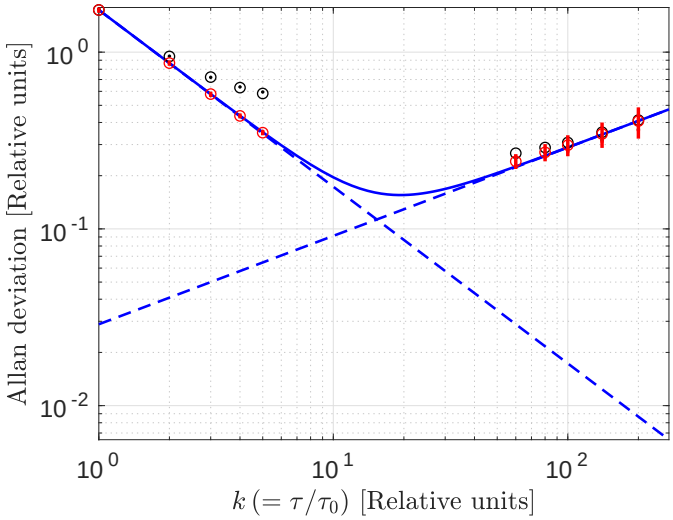

Fig. 18. Stability analysis for the WPM plus RWFM noise with blocks of missing data shown in Fig. 17. The dashed blue lines represent the Allan deviation for WPM and RWFM in the full data case, whereas their sum, obtained through (90), is the solid blue line. The corrected Allan deviation (red circles) removes the bias of the Allan deviation without correction (black circles) in the WPM region (small observation interval values), and reduces it in the RWFM region (large observation interval values). The red and black dots are estimates of the Allan deviation with and without correction, respectively. The red bars are 95% confidence intervals.

observation interval region, where no noise dominates. The bias of the Allan deviation without correction for WPM is completely removed, whereas the smaller bias of the Allan deviation without correction for RWFM is reduced.

3) WFM-RWFM: Figure 19 shows the frequency deviation for the sum of a WFM and an RWFM with the pattern of missing data blocks described at the beginning of Sect. IV-B. The corresponding stability analysis is displayed in Fig. 20. The dashed blue lines with slopes $\tau^{-1/2}$ ($k^{-1/2}$ in discrete time) and $\tau^{1/2}$ ($k^{1/2}$ in discrete time) represent the Allan deviation for WFM and RWFM when all of the data are available, respectively, whereas their sum, obtained thorough

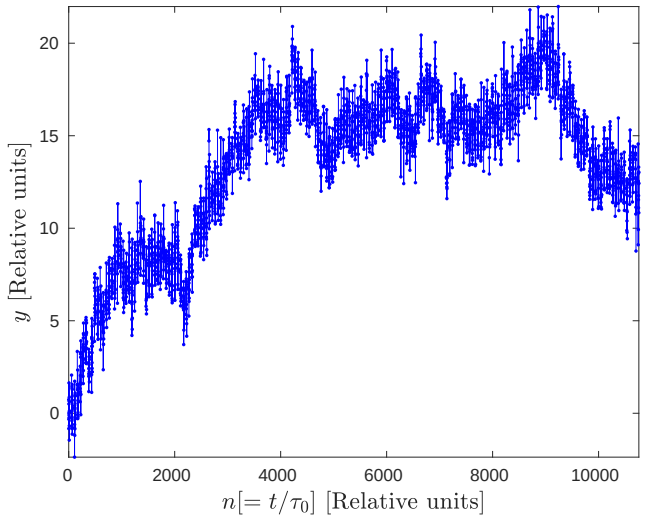

Fig. 19. Simulated frequency measurements for the sum of WFM and RWFM with blocks of missing data. This pattern of missing data is described in detail at the beginning of Sect. IV-B.

(90), is represented by the solid blue line. The Allan deviation for missing data without correction is represented by the black circles, and the corrected Allan deviation for missing data by the red circles. Estimates of the Allan deviation without correction and of the corrected Allan deviation are represented by black and red dots, respectively. The red bars are 95% confidence intervals. The correction is computed for WFM at small observation interval values, where WFM dominates, and for RWFM for large observation interval values, where RWFM dominates. Similarly to the previous cases, the correction is not computed for intermediate observation interval values, where a dominant noise does not exist. The picture shows that the corrected Allan deviation completely removes the bias in the WFM region, and it reduces the smaller bias in the RWFM region, resulting in a negligible bias.

C. Choosing Wrong Noise Components

As previously mentioned, the only way to correct the mathematical definition of the Allan variance is by introducing a correction factor which depends on the type of noise component dominating in every observation interval region. The correction factor is not computed in the transition regions where a dominant noise does not exist. Consequently, the corrected Allan variance is a parametric estimator based on a stochastic model of the data. The parameters of the model are the types of noise components and the corresponding dominance regions. As in any parametric estimator, when the wrong model is used, the corresponding estimation results can have poor performances. Fortunately, the analysis of the obtained results can be used to decide if a model mismatch occurred. This concept is better illustrated through an example.

Fig. 21 shows frequency measurements made by the sum of a WFM and an RWFM with blocks of missing data. The percentage of missing data is 94%, and the pattern of missing data is described at the beginning of Sect. IV-A. Figure 22 shows, for the full data case, the Allan deviation

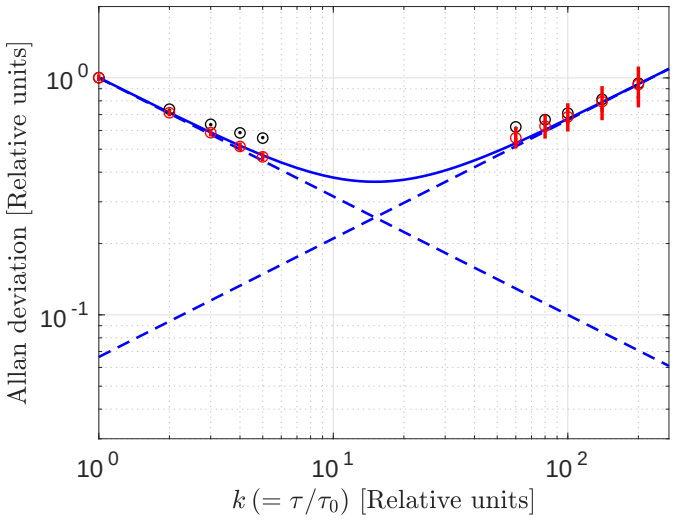

Fig. 20. Stability analysis for the WFM plus RWFM noise with blocks of missing data shown in Fig. 19. The Allan deviation for WFM and RWFM in the full data case is represented by the dashed blue lines, whereas their sum, obtained through (90), is the solid blue line. The corrected Allan deviation (red circles) completely removes the bias of the Allan deviation without correction (black circles) for WFM (short observation interval values), and reduces the bias for RWFM (large observation interval values). The red and black circles are estimates of the Allan deviation with and without correction, respectively. The red bars are 95% confidence intervals.

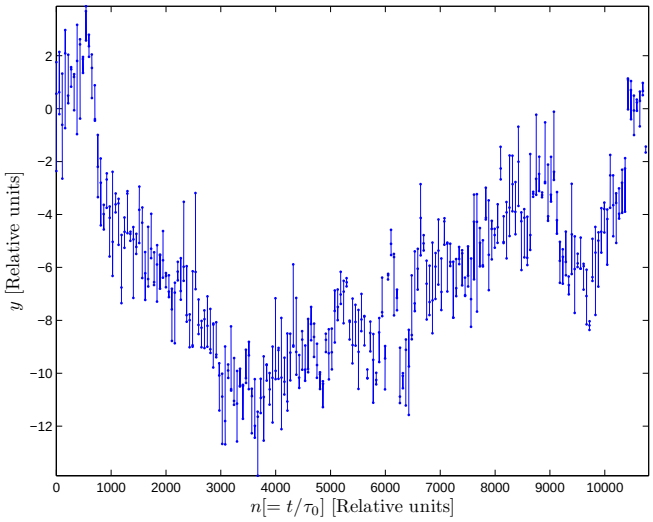

Fig. 21. Simulated frequency measurements for the sum of a WFM and an RWFM with blocks of missing data. This pattern of missing data is described in detail at the beginning of Sect. IV-B.

for WFM (dashed blue line with $k^{-1/2}$ slope), for RWFM (dashed blue line with slope $k^{1/2}$), and for the sum of them (solid blue line), obtained through 90. The solid red line represents the corrected Allan deviation obtained when the wrong noise components are selected. In the short observation interval region where WFM dominates, in fact, the correction is computed for RWFM, whereas in the large observation interval region where RWFM dominates, the correction is computed for WFM. The obtained corrected Allan deviation has large estimation errors. It is immediately clear, though, that a model mismatch occurred, because the estimated Allan deviation is not consistent with the the *bathtub diagram* shown in Fig. 23. A proper Allan deviation must in fact follow the convex function in this diagram (provided that all deterministic components, such as frequency drifts, have been removed). Since the corrected Allan deviation in Fig. 22 is a non-convex function, it does not represent a proper Allan deviation, and hence the wrong noise model has been used. The consistency between the corrected Allan deviation and the bathtub diagram could be used to design a model mismatch detector, as it is done in several fields, such as, for instance, radar detection [17], machine learning [18], and chemical engineering [19].

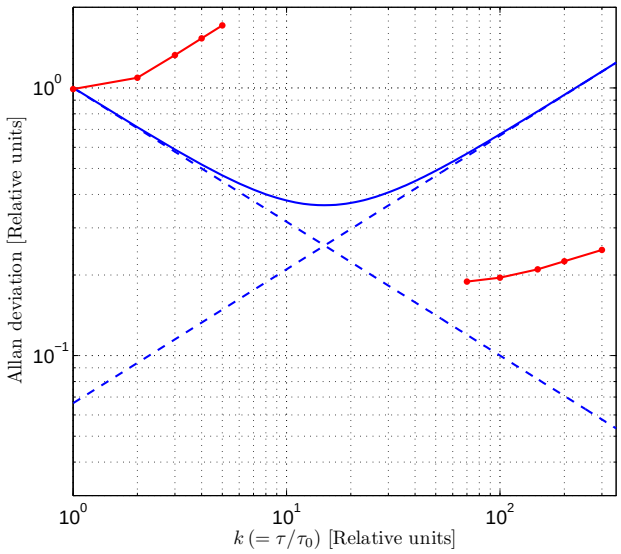

Fig. 22. Stability analysis for the WFM plus RWFM noise with blocks of missing data shown in Fig. 21. The dashed blue lines represent the Allan deviation of the WFM and RWFM noise components for the full data case ($k^{-1/2}$ and $k^{1/2}$ slopes, respectively), whereas their sum, obtained through (90), is the solid blue line. The corrected Allan deviation (red line) is a poor estimate of the desired full data case, because the correction is wrongly computed for RWFM in the short observation interval region, where WFM dominates, and for WFM in the large observation interval region, where RWFM dominates. This model mismatch is clearly revealed by the disagreement with the convex behavior of the bathtub diagram in Fig. 23, which any proper Allan deviation must follow.

V. Conclusions

The Allan variance computed from frequency measurements with missing data can be profoundly different from the full data case. This difference, referred to as bias, can be corrected by modifying the definition of the Allan variance. The corrected Allan variance eliminates the bias, or largely reduces it, and, on the average, returns the Allan variance behavior expected for the full data case. This article shows how to correct the Allan variance for WFM, WPM, and RWFM, three

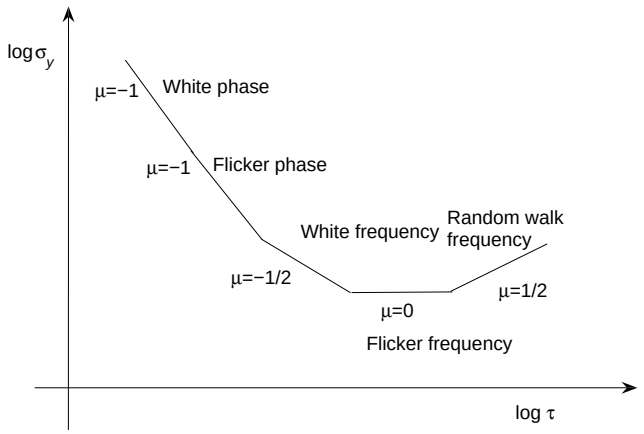

Fig. 23. Bathtub diagram. Any proper Allan deviation must follow this convex function, whose actual shape depends on the type of noise components present in the considered measurements. The Allan deviation for each individual noise component is proportional to τ^{μ}, and therefore becomes a straight line in the bilogarithmic representation.

of the most common noise components of atomic clocks. The performances of the corrected Allan variance are validated through Monte Carlo simulations. When multiple noise components are present, the corrected Allan variance is an effective approximation of the expected Allan variance in the observation interval regions where a dominant noise is present. The corrected Allan variance can be also straightforwardly embedded in the dynamic Allan variance (DAVAR) [12]-[15], and the resulting corrected DAVAR can be used to perform time-varying stability analysis when nonstationary frequency measurements with missing data are considered.

Note that it would be interesting to extend the developed method to other relevant quantities used in precise timing, such as, for instance, the modified Allan variance (MVAR), the Hadamard variance (HVAR), and the time deviation (TDEV). Similarly, extensions to other noise components, such as flicker phase modulation (FPM) and flicker frequency modulation (FFM), are of interest. Finally, the characterization of the corrected Allan variance in presence of deterministic periodic components is a topic which deserves further investigation.

VI. Appendix 1: Allan Variance for WFM

The Allan variance for the WFM defined in Sect. II-A1 can be derived by using the form (10). It is

$$E[y_k^2[n+k]] = E\left[\left(\frac{1}{k}\sum_{m=1}^{k} y[n+m]\right)^2\right] \tag{91}$$

$$= \frac{1}{k^2}\sum_{m'=1}^{k}\sum_{m''=1}^{k} E\left[y[n+m']y[n+m'']\right] \tag{92}$$

From (19), when $n+m' \neq n+m''$, then $E\left[y[n+m']y[n+m'']\right] = 0$, therefore

$$E[y_k^2[n+k]] = \frac{1}{k^2}\sum_{m=1}^{k} E[y^2[n+m]] \tag{93}$$

Since, from (18), $E[y^2[n+m]] = \sigma^2/\tau_0$ regardless of the n and m values, it is

$$E[y_k^2[n+k]] = \frac{\sigma^2}{k\tau_0} \tag{94}$$

Similarly

$$E[y_k^2[n]] = \frac{\sigma^2}{k\tau_0} \tag{95}$$

From (8) and (9),

$$E[y_k[n+k]y_k[n]] = \frac{1}{k^2}\sum_{m'=1}^{k}\sum_{m''=1}^{k} E[y[n+m']y[n-m''+1]] \tag{96}$$

But $n+m' > n-m''+1$, for $m', m'' = 1, \ldots, k$, therefore, from (19),

$$E[y[n+m']y[n-m''+1]] = 0 \tag{97}$$

and, consequently,

$$E[y_k[n+k]y_k[n]] = 0 \tag{98}$$

By using (94), (95), and (98), it is

$$E\left[\left(y_k[n+k] - y_k[n]\right)^2\right] = \frac{2\sigma^2}{k\tau_0} \tag{99}$$

Therefore, replacing in (7),

$$\sigma_y^2[k] = \frac{1}{2}\frac{1}{N-2k+1}\sum_{n=k}^{N-k}\frac{2\sigma^2}{k\tau_0} \tag{100}$$

$$= \frac{\sigma^2}{k\tau_0} \tag{101}$$

whose corresponding Allan deviation is (20).

VII. Appendix 2: Allan Variance for WPM

The Allan variance for the WPM defined in Sect. II-A2 can be obtained by using the form (14). It is

$$E\left[\left(x[n+k] - 2x[n] + x[n-k]\right)^2\right] = E[x^2[n+k]] + 4E[x^2[n]] + E[x^2[n-k]] - 4E[x[n+k]x[n]] + 2E[x[n+k]x[n-k]] - 4E[x[n]x[n-k]] \tag{102}$$

From (23),

$$E[x^2[n+k]] = E[x^2[n]] = E[x^2[n-k]] = \sigma^2 \tag{103}$$

whereas, from (24), and by noting that $k \geq 1$,

$$E[x[n+k]x[n]] = E[x[n+k]x[n-k]] = E[x[n]x[n-k]] = 0 \tag{104}$$

By comparing (7) and (14), it is

$$E\left[\left(y_k[n+k] - y_k[n]\right)^2\right] = \frac{E\left[\left(x[n+k] - 2x[n] + x[n-k]\right)^2\right]}{k^2\tau_0^2} \tag{105}$$

By using (102)-(104),

$$E\left[(y_k[n+k]-y_k[n])^2\right]=\frac{6\sigma^2}{k^2\tau_0^2} \tag{106}$$

Replacing in (14),

$$\sigma_y^2[k]=\frac{1}{2}\frac{1}{N-2k+1}\sum_{n=k}^{N-k}\frac{6\sigma^2}{k^2\tau_0^2} \tag{107}$$

$$=\frac{3\sigma^2}{k^2\tau_0^2} \tag{108}$$

whose corresponding Allan deviation is (28).

VIII. Appendix 3: Allan Variance for RWFM

The Allan variance for the RWFM defined in Sect. II-A3 can be derived by using the form (10). First, it is useful to derive the autocorrelation function of the normalized frequency deviation $y(t)$,

$$R_y(t',t'')=E[y(t')y(t'')] \tag{109}$$

$$=\int_0^{t'}\int_0^{t''}E[\xi(t')\xi(t'')]dt'dt'' \tag{110}$$

Replacing $E[\xi(t')\xi(t'')]$ from (32),

$$R_y(t',t'')=\sigma^2\int_0^{t'}\int_0^{t''}\delta(t'-t'')dt'dt'' \tag{111}$$

When $t''<t'$,

$$R_y(t',t'')=\sigma^2\int_0^{t''}\int_0^{t''}\delta(t'-t'')dt'dt'' \tag{112}$$

$$=\sigma^2 t'' \tag{113}$$

Similarly, when $t'<t''$,

$$R_y(t',t'')=\sigma^2 t' \tag{114}$$

Combining these two results, we obtain

$$R_y(t',t'')=\sigma^2\min(t',t'') \tag{115}$$

Then, by using (5), the variance of the frequency measurement $y[n]$ is given by

$$E[y^2[n]]=E\left[\left(\frac{1}{\tau_0}\int_{(n-1)\tau_0}^{n\tau_0}y(t)dt\right)^2\right] \tag{116}$$

$$=\frac{1}{\tau_0^2}\iint_{(n-1)\tau_0}^{n\tau_0}E[y(t')y(t'')]dt'dt'' \tag{117}$$

Replacing (115),

$$E[y^2[n]]=\frac{\sigma^2}{\tau_0^2}\iint_{(n-1)\tau_0}^{n\tau_0}\min(t',t'')dt'dt'' \tag{118}$$

In the half plane where $t''<t'$, the double integral becomes

$$\iint_{(n-1)\tau_0}^{n\tau_0}t''dt'dt''=\frac{\tau_0^3}{6}(3n-2) \tag{119}$$

The identical result is obtained in the half plane where $t'\le t''$, and since the integral values for the two half planes add up, it is

$$E[y^2[n]]=\frac{\sigma^2}{\tau_0^2}2\frac{\tau_0^3}{6}(3n-2) \tag{120}$$

Simplifying

$$E[y^2[n]]=\sigma^2\tau_0\left(n-\frac{2}{3}\right) \tag{121}$$

which corresponds to (34). The same approach leads to

$$E[y[n]y[m]]=\frac{\sigma^2}{\tau_0^2}\int_{(n-1)\tau_0}^{n\tau_0}\int_{(m-1)\tau_0}^{m\tau_0}\min(t',t'')dt'dt'' \tag{122}$$

When $m<n$,

$$E[y[n]y[m]]=\frac{\sigma^2}{\tau_0^2}\int_{(n-1)\tau_0}^{n\tau_0}\int_{(m-1)\tau_0}^{m\tau_0}t''dt'dt'' \tag{123}$$

$$=\sigma^2\tau_0\left(m-\frac{1}{2}\right) \tag{124}$$

Similarly, when $n<m$,

$$E[y[n]y[m]]=\frac{\sigma^2}{\tau_0^2}\int_{(n-1)\tau_0}^{n\tau_0}\int_{(m-1)\tau_0}^{m\tau_0}t'dt'dt'' \tag{125}$$

$$=\sigma^2\tau_0\left(n-\frac{1}{2}\right) \tag{126}$$

Combining the two results,

$$E[y[n]y[m]]=\sigma^2\tau_0\left(\min(n,m)-\frac{1}{2}\right) \tag{127}$$

which is (35).

Now that $E[y^2[n]]$ and $E[y[n]y[m]]$ are known, the terms $E[y_k^2[n+k]]$, $E[y_k^2[n]]$, and $E[y_k[n+k]y_k[n]]$ in (10) can be evaluated. It is

$$E[y_k^2[n+k]]=E\left[\left(\frac{1}{k}\sum_{m=1}^{k}y[n+m]\right)^2\right] \tag{128}$$

$$=\frac{1}{k^2}\sum_{m'=1}^{k}\sum_{m''=1}^{k}E[y[n+m']y[n+m'']] \tag{129}$$

$$=\frac{1}{k^2}E[y^2[n+m]]+\frac{1}{k^2}\sum_{\substack{m'=1\\m'\neq m''}}^{k}\sum_{m''=1}^{k}E[y[n+m']y[n+m'']] \tag{130}$$

Replacing (118) and (127),

$$E[y_k^2[n+k]]=\frac{\sigma^2\tau_0}{k^2}\sum_{m=1}^{k}\left(n+m-\frac{2}{3}\right)+\frac{\sigma^2\tau_0}{k^2}\sum_{\substack{m'=1\\m'\neq m''}}^{k}\sum_{m''=1}^{k}\left(\min(n+m',n+m'')-\frac{1}{2}\right) \tag{131}$$

These summations can be solved exactly, giving

$$E[y_k^2[n+k]]=\sigma^2\tau_0\left(n+\frac{k}{3}\right) \tag{132}$$

With the identical procedure, one obtains

$$E[y_k^2[n]] = \sigma^2\tau_0\left(n - \frac{2}{3}k\right) \tag{133}$$

and

$$E[y_k[n+k]y_k[n]] = \sigma^2\tau_0\left(n - \frac{k}{2}\right) \tag{134}$$

By using (132)-(134), one has that

$$E\left[\left(y_k[n+k] - y_k[n]\right)^2\right] = \frac{2}{3}\sigma^2 k\tau_0 \tag{135}$$

Substituting in (10), it is

$$\sigma_y^2[k] = \frac{1}{3}\sigma^2 k\tau_0 \tag{136}$$

whose corresponding Allan deviation is (36).

IX. Appendix 4: Bias of the Allan Variance Estimator for Time Measurements With Missing Data

The Allan variance for time measurements with full data (14) can be written as

$$\sigma_y^2[k] = \frac{1}{2}\frac{1}{N-2k+1}\sum_{n=k}^{N-k}\frac{E[\Delta^2[n,k]]}{k^2\tau_0^2} \tag{137}$$

where $\Delta[n,k] = x[n+k] - 2x[n] + x[n-k]$. For common clock noise components it is

$$E[\Delta^2[n,k]] = E[\Delta^2[k]] \tag{138}$$

therefore

$$\sigma_y^2[k] = \frac{1}{2}\frac{E[\Delta^2[k]]}{k^2\tau_0^2} \tag{139}$$

In case of missing data, equivalently to (43) and (137), the estimator (15) can be written as

$$\hat{\sigma}_y^2[k] = \frac{1}{2}\frac{1}{\#I'(k)}\sum_{n\in I'(k)}\frac{\Delta^2[n,k]}{k^2\tau_0^2} \tag{140}$$

where $I'(k)$ is the set of discrete time values n at which the triplet $x[n+k]$, $x[n]$, $x[n-k]$ is available for the given k. If no triplet is available, then $I'(k)$ is the empty set and $\hat{\sigma}_y^2[k]$ is not defined for the given k. The corresponding expected value is given by

$$E[\hat{\sigma}_y^2[k]] = \frac{1}{2}\frac{1}{\#I'(k)}\sum_{n\in I'(k)}\frac{E[\Delta^2[n,k]]}{k^2\tau_0^2} \tag{141}$$

Replacing (138) gives (139). Therefore, *for time measurements*,

$$E[\hat{\sigma}_y^2[k]] \text{ (Missing data)} = \sigma_y^2[k] \text{ (Full data)} \tag{142}$$

and, consequently, the Allan variance estimator for time measurements with missing data is unbiased.

X. Appendix 5: Allan Variance for Multiple Noise Components

If

$$y(t) = y_{\text{WFM}}(t) + y_{\text{WPM}}(t) \tag{143}$$

where $y_{\text{WFM}}(t)$ and $y_{\text{WPM}}(t)$ are statistically independent noise components, then, by using (5), it is

$$y[n] = y_{\text{WFM}}[n] + y_{\text{WPM}}[n] \tag{144}$$

and, consequently, from (9),

$$y_k[n] = y_{k,\text{WFM}}[n] + y_{k,\text{WPM}}[n] \tag{145}$$

The corresponding Allan variance becomes

$$\sigma_y^2[k] = \frac{1}{2}\frac{1}{N-2k+1}\sum_{n=k}^{N-k} E\left[\left(y_{k,\text{WFM}}[n+k] + y_{k,\text{WPM}}[n+k] - y_{k,\text{WFM}}[n] - y_{k,\text{WPM}}[n]\right)^2\right] \tag{146}$$

Since $y_{\text{WFM}}(t)$ and $y_{\text{WPM}}(t)$ are statistically independent noise components with zero mean, then

$$E\left[y_{k,\text{WFM}}[n+k]y_{k,\text{WPM}}[n+k]\right] = 0 \tag{147}$$

$$E\left[y_{k,\text{WFM}}[n+k]y_{k,\text{WPM}}[n]\right] = 0 \tag{148}$$

$$E\left[y_{k,\text{WPM}}[n+k]y_{k,\text{WFM}}[n]\right] = 0 \tag{149}$$

Substituting,

$$\sigma_y^2[k] = \sigma_{y,\text{WFM}}^2[k] + \sigma_{y,\text{WPM}}^2[k] \tag{150}$$

where $\sigma_{y,\text{WFM}}^2[k]$ and $\sigma_{y,\text{WPM}}^2[k]$ are the Allan variances of the individual noise components WFM and WPM, respectively. This result corresponds to (84) and holds for any sum of statistically independent noise components with zero mean.

XI. Appendix 6: Corrected Allan Variance for Multiple Noise Components

Suppose that, as in Appendix 5, $y(t) = y_{\text{WFM}}(t) + y_{\text{WPM}}(t)$, where $y_{\text{WFM}}(t)$ and $y_{\text{WPM}}(t)$ are statistically independent noise components. In case of missing data, the corresponding Allan variance (146), corrected for WFM, is

$$\sigma_y^2[k] \text{ (Corrected)} = \frac{1}{2}\frac{1}{\#I(k)}\sum_{n\in I(k)}\alpha_{\text{WFM}}^2(n,k) \times E\left[\left(y'_{k,\text{WFM}}[n+k] + y'_{k,\text{WPM}}[n+k] - y'_{k,\text{WFM}}[n] - y'_{k,\text{WPM}}[n]\right)^2\right] \tag{151}$$

Since (147) holds, the corrected Allan variance can be written as

$$\sigma_y^2[k] \text{ (Corrected)} = \frac{1}{2}\frac{1}{\#I(k)}\sum_{n\in I(k)}\alpha_{\text{WFM}}^2(n,k) \times E\left[\left(y'_{k,\text{WFM}}[n+k] - y'_{k,\text{WFM}}[n]\right)^2\right] + \frac{1}{2}\frac{1}{\#I(k)}\sum_{n\in I(k)}\alpha_{\text{WFM}}^2(n,k) \times E\left[\left(y'_{k,\text{WPM}}[n+k] - y'_{k,\text{WPM}}[n]\right)^2\right] \tag{152}$$

Equivalently,

$$\sigma_y^2[k] \text{ (Corrected)} = \sigma_{y,\text{WFM}}^2[k] \text{ (Full data)} + \sigma_{y,\text{WPM}}^2[k] \text{ (Corrected for WFM)} \quad (153)$$

The mixed term $\sigma_{y,\text{WPM}}^2[k]$ (Corrected for WFM) represents the Allan variance of a WPM with missing data, corrected for WFM rather than for WPM. This result corresponds to (86).

REFERENCES

[1] D. W. Allan, "Statistics of atomic frequency standards," *Proc. IEEE*, vol. 54, no. 2, pp. 221-230, 1966.

[2] D. W. Allan, "Time and Frequency (Time-Domain) Characterization, Estimation, and Prediction of Precision Clocks and Oscillators," *IEEE Trans. Ultra. Ferro. Freq. Contr.*, vol. 34, no. 6, pp. 647-654, 1987.

[3] IEEE Standard Definitions of Physical Quantities for Fundamental Frequency and Time Metrology, IEEE Std. 1139-1999.

[4] ITU-R Recommendation TF 538-3, "Measures for random instabilities in frequency and time (phase)," *International Telecommunication Union – Radiocommunication ITU-R*, vol. 2000, TF Series, Geneva, 2001.

[5] L. Cacciapuoti and C. Salomon, "Atomic Clock Ensemble in Space," *Journal of Physics: Conference Series*, vol. 327, no. 1, pp. 1-13, 2011.

[6] I. Sesia, E. Cantoni, A. Cernigliaro, G. Signorile, G. Fantino, and P. Tavella, "An Efficient and Configurable Preprocessing Algorithm to Improve Stability Analysis," *IEEE Trans. Ultra. Ferro. Freq. Contr.*, vol. 63, no. 4, pp. 575-581, April 2016.

[7] S. M. Kay, *Fundamentals of Statistical Signal Processing: Estimation Theory*, Prentice-Hall, 1993.

[8] I. Sesia and P. Tavella, "The Allan variance for measurements with long periods of missing data and outliers," *Metrologia*, vol. 45, no. 6, pp. 134-142, Dec. 2008.

[9] P. Kartaschoff, *Frequency and Time*, Academic Press, New York, 1978.

[10] C. Hackman and T. E. Parker, "Noise analysis of unevenly spaced time series data," *Metrologia*, vol. 33, pp. 457-466, 1996.

[11] P. Tavella, "Statistical and mathematical tools for atomic clocks," *Metrologia*, vol. 45, no. 6, pp. S183-S192, December 2008.

[12] L. Galleani and P. Tavella, "The Dynamic Allan Variance," *IEEE Trans. Ultra. Ferro. Freq. Contr.*, vol. 56, no. 3, pp. 450-464, 2009.

[13] L. Galleani, "The Dynamic Allan Variance II: A Fast Computational Algorithm," *IEEE Trans. Ultra. Ferro. Freq. Contr.*, vol. 57, no. 1, pp. 182-188, 2010.

[14] L. Galleani and P. Tavella, "The Dynamic Allan Variance V: Recent Advances in Dynamic Stability Analysis," *IEEE Trans. Ultra. Ferro. Freq. Contr.*, vol. 63, no. 4, pp. 624-635, April 2016.

[15] I. Sesia, L. Galleani, and P. Tavella, "Application of the Dynamic Allan Variance for the Characterization of Space Clock Behavior," *IEEE Trans. Aero. Elec. Sys.*, vol. 47, no. 2, pp. 884-895, Apr. 2011.

[16] L. Galleani and I. Sesia, "Estimating the Allan variance from frequency measurements with missing data," *IFCS-EFTF 2017*, 9-13 July 2017, Besancon, France.

[17] S. Fortunati, F. Gini, and M. S. Greco, "Parameter Bounds Under Misspecified Models for Adaptive Radar Detection," in R. Chellappa and S. Theodoridis, *Academic Press Library in Signal Processing, Volume 7: Array, Radar and Communications Engineering*, Academic Press, 2018.

[18] A. Roy, H. Xu, and S. Pokutta, "Reinforcement learning under model mismatch," *31st Annual Conference on Neural Information Processing Systems - NIPS 2017*, 4-9 December 2017, Long Beach, United States.

[19] N. Meneghetti, P. Facco, F. Bezzo, and M. Barolo, "Diagnosing Process/Model Mismatch in First-Principles Models by Latent Variable Modeling," *Computer Aided Chemical Engineering*, vol. 33, pp. 1897-1902, 2014.